TISSUE ENGINEERING: Part C
Volume 16, Number 3, 2010

DOI: 10.1089/ten.tec.2009.0020

Evaluation of Early Osteochondral Defect Repair in a Rabbit Model Utilizing Fourier Transform–Infrared Imaging Spectroscopy, Magnetic Resonance Imaging, and Quantitative T2 Mapping

Minwook Kim, M.S.,[1] Li F. Foo, M.D.,[2] Christopher Uggen, M.D.,[3] Steven Lyman, Ph.D.,[4] James T. Ryaby, Ph.D.,[5] Daniel P. Moynihan, M.D.,[3] Daniel Anthony Grande, Ph.D.,[3] Hollis G. Potter, M.D.,[2] and Nancy Pleshko, Ph.D.[1]

Context: Evaluation of the morphology and matrix composition of repair cartilage is a critical step toward understanding the natural history of cartilage repair and efficacy of potential therapeutics. In the current study, short-term articular cartilage repair (3 and 6 weeks) was evaluated in a rabbit osteochondral defect model treated with thrombin peptide (TP-508) using magnetic resonance imaging (MRI), quantitative T2 mapping, and Fourier transform–infrared imaging spectroscopy (FT-IRIS).

Methods: Three-mm-diameter osteochondral defects were made in the rabbit trochlear groove and filled with either TP-508 plus poly-lactoglycolidic acid microspheres or poly-lactoglycolidic acid microspheres alone (placebo). Repair tissue and adjacent normal cartilage were evaluated at 3 and 6 weeks postdefect creation. Intact knees were evaluated by magnetic resonance imaging for repair morphology, and with quantitative T2 mapping to assess collagen orientation. Histological sections were evaluated by FT-IRIS for parameters that reflect collagen quantity and quality, as well as proteoglycan (PG) content.

Results and Conclusion: There was no significant difference in volume of repair tissue at either time point. At 6 weeks, placebo repair tissue demonstrated longer T2 values ($p < 0.01$) than TP-508 did. Although both placebo and TP-508 repair tissue demonstrated longer T2 values than adjacent normal cartilage did, the 6-week T2 values of the TP-508 specimens were closer to those of the adjacent normal cartilage than were the placebo values. FT-IRIS analysis demonstrated a significant increase in collagen content, integrity, and PG content of the TP-508 repair tissue from 3 to 6 weeks ($p \leq 0.05$). In addition, the collagen and PG content of the TP-508 samples were closer to normal cartilage at 3 weeks than were the placebo samples. Further, there was a significant inverse correlation between the T2 relaxation values and collagen orientation in the normal cartilage. However, there were no significant correlations between T2 relaxation values and any FT-IRIS parameter in the repair tissue. Together, the data demonstrate that MRI and FT-IRIS assessment of cartilage repair tissue provide molecular information that furthers understanding of the cartilage repair process.

Introduction

Articular cartilage provides a lubricating surface at the end of diarthrodial joints that permits pain-free movement in normal individuals.[1,2] The repair of traumatic chondral defects or osteoarthritic cartilage degradation has remained an area of extensive and active research in orthopaedics.[3,4] Cell-based strategies for cartilage repair procedures have utilized chondrocytes,[5–8] chondrocyte precursor cells, periosteum,[9,10] perichondrium,[11,12] and marrow-derived cells[13] with and without growth factors.[14,15] Surgical techniques for repair including both autologous and allogenic osteochondral graft transplantation,[16] microfracture chondroplasty,[17] and other similar techniques have been employed with some success. In spite of these advances, a technique that enables formation of repair tissue properties similar to native hyaline articular cartilage remains elusive.

As sophisticated strategies and various biomaterials are increasingly utilized to restore cartilage defects, objective methods of articular cartilage evaluation have become progressively

[1]Musculoskeletal Imaging & Spectroscopy Laboratory, Hospital for Special Surgery, New York, New York.
[2]Department of Radiology and Imaging, Hospital for Special Surgery, New York, New York.
[3]North Shore/LIJ Medical Center, New Hyde Park, New York.
[4]Outcomes Research, Hospital for Special Surgery, New York, New York.
[5]Ryaby Associates LLC, Scottsdale, Arizona.

more important. Advances in magnetic resonance imaging (MRI) presently allow for objective and noninvasive assessment of repair cartilage morphology, as well as providing semiquantitative assessment of the extracellular matrix.[18,19] Although MRI parameters such as quantitative T2 values are sensitive to overall cartilage matrix composition,[20] few MRI parameters have been definitively correlated to specific matrix molecular components.

Fourier transform infrared imaging spectroscopy (FT-IRIS) has emerged as a novel imaging modality and has recently been utilized to evaluate biological tissues, including cartilage[21–24] and bone,[25,26] as well as engineered cartilaginous tissue[27] and biomaterials such as polymeric hydrogels.[28] FT-IRIS combines an FTIR spectrometer and light microscope, and thus permits identification of the tissue components and their distribution and orientation within the tissue.[28] In cartilaginous tissues, semiquantification of collagen and proteoglycan (PG) content, collagen integrity (related to helical integrity), and stratification of collagen fibril network orientation[29] have been demonstrated with this technique.

In the current study, we used a well-described rabbit model[30] of surgically created osteochondral defects treated with either carrier control or the synthetic thrombin peptide (TP-508) delivered within the carrier. Recent studies using TP-508 have demonstrated enhanced dermal wound repair,[31] corneal epithelial repair,[32] as well as increased fracture repair.[33] The synthetic peptide binds to high-affinity thrombin receptors and modulates thrombin mitogenesis.[34] Evaluation of cartilage repair was performed at short-term follow-up of 3- and 6-week time points utilizing MRI, quantitative T2 mapping, and FT-IRIS. Correlations were also made between the imaging techniques. We hypothesized that the use of TP-508 in cartilage repair would result in production of matrix that is more similar to normal native hyaline cartilage than that formed with placebo carrier alone. Further, we demonstrate that use of FT-IRIS in conjunction with MRI enhances understanding of the cartilage repair process.

Materials and Methods

Surgical procedure

All surgical procedures were performed under IACUC-approved protocols at the Feinstein Institute for Medical Research (Manhasset, NY). A total of 17 adult male New Zealand White rabbits were enrolled in this study. All animals were 8 months of age and weighed greater than 4.5 kg. The animals underwent bilateral knee arthrotomies under general anesthesia induced by administration of intramuscular injection ketamine (35 mg/kg) and xylazine (5 mg/kg). A medial parapatellar approach was used to enter the knee joint, and the patella was laterally dislocated to expose the articular surface of the distal femur and trochlear groove. Under sterile techniques, a 3-mm-diameter, 2.5-mm-deep osteochondral defect was made in the central flattened region of the trochlear groove, 1 cm distal to the fused distal femoral growth plate, using a pneumatic drill under saline irrigation.

Implant preparation and delivery

TP-508 was incorporated into 100 μm poly-lactoglycolidic acid (PLGA) microspheres at a concentration of 50 μg/100 μL. Unilateral trochlear defects were filled with the peptide-containing microspheres immobilized in dextran via pipette, and the articular surface smoothed to form a congruent surface. Defects in the opposite knee were filled with nonpeptide-containing PLGA microspheres in dextran (placebo controls). The patella was reduced, and the incision wound closed in layers with 4-0 Vicryl sutures. Animals were allowed unrestricted activity postoperatively. Antibiotics and analgesics were administered perioperatively as per Institutional Animal Care and Use Committee (IACUC) protocol. Animals were sacrificed at 3 ($n = 6$) and 6 ($n = 11$) weeks after surgery, and knee joints harvested for imaging.

Magnetic resonance imaging

MRI was performed on a 3 tesla clinical imaging system (GE Healthcare, Milwaukee WI), using a prototype 2×7 cm solenoid birdcage coil (GE Healthcare).

Morphologic imaging was performed using a cartilage-sensitive fast spin echo sequence in the axial and sagittal planes. These were acquired with repetition time of 4300 ms, echo time of 25–30 ms (effective), echo train length of 11, and spatial resolution of 156 μm (frequency)×156 μm (phase)× 1 mm, at three excitations. These pulse sequence parameters had been previously used to assess cartilage repair in a canine model.[35]

Quantitative T2 mapping (GE Healthcare) was performed using a multislice, multiecho modified Carr-Purcell-Meiboom-Gill (CPMG) pulse sequence that utilizes interleaved slices and tailored refocusing pulses to minimize contribution from stimulated echoes.[36] Eight echoes were sampled—sequential multiples of the first echo time (9–10 ms), at a repetition time of 800 ms; in-plane resolution of 208.3 μm (frequency)×312.5 μm (phase)×1 mm, at two excitations. After image acquisition, datasets were analyzed on a pixel-by-pixel basis with a two-parameter-weighted least-squares fit (Functool 3.1; GE Healthcare), assuming a monoexponential decay. Quantitative T2 values were calculated by taking the natural logarithm of the signal decay curve in a selected region of interest (ROI). ROIs were obtained in a standardized fashion, within a fixed area in the center of the repair and normal cartilage that was not immediately at the interface with the repair tissue.

FT-IRIS

Tissue processing. After MRI, the knee joints were dissected and distal femurs fixed in 80% EtOH and 1% cetylpyridinium chloride for 24 h, and decalcified in EDTA solution for 2 weeks. Tissues were then embedded in paraffin and sectioned at 7 μm thickness. One or two sections per tissue were mounted onto barium fluoride windows for FT-IRIS.

Data collection. FT-IRIS was performed using a Spectrum Spotlight 300 spectrometer (Perkin-Elmer, Waltham, MA). A rectangular ROI that contained the defect and adjacent cartilage was selected, and the data were acquired at a spatial resolution of 25 μm and spectral resolution of 4 cm^{-1}. Imaging data were analyzed using ISys 3.1 software (Spectral Dimensions, Olney, MD). FT-IRIS-specific parameters of cartilage constituents, collagen, and PG were calculated as previously described.[21] The integrated absorbances at 1594–1718 cm^{-1} (collagen–amide Am I: C=O stretch), 1490–1594 cm^{-1} (collagen–Am II: C–N stretch associated with N–H bend), 1326–1356 cm^{-1} (side chain rotation), and

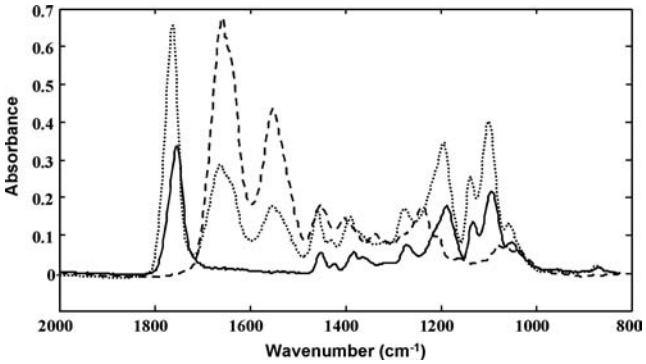

FIG. 1. Infrared spectra of pure poly-lactoglycolidic acid (PLGA) (solid line), normal cartilage (dashed line), and PLGA contribution in repair cartilage (dotted line).

958–1144 cm^{-1} (sugar-PG: C–O–C and C–OH ring vibrations) were calculated. Ratios of integrated areas were used to compare the relative quantity of PG/Am I and 1338/Am II (collagen integrity). These values were calculated for both repair tissue and adjacent normal cartilage. The integrated area of the PLGA absorbance from 1792 to 1730 cm^{-1} was utilized to monitor the quantity and distribution of PLGA, and the absorbances that arise from PLGA in the PG region were spectrally subtracted (Fig. 1). Polarized FT-IRIS was utilized to assess collagen fibril orientation.[29] The orientation of collagen fibrils was determined by the ratio of Am I and Am II at 0° polarization. Based on this parameter, a ratio $\geq$2.7 reflects fibrils aligned parallel to the articular surface; $\leq$1.7, fibrils perpendicular to the articular surface, and 2.7–1.7, a random or mixed fibril orientation. For quantitative analysis, pixels in the polarized FT-IRIS image for normal and repair cartilage, respectively, were divided into three orientation categories as described above, and the percentage of pixels falling into each category was calculated.

Histological analysis

Six-micrometer sections were stained with alcian blue for PG content,[37] and Bioquant software (Bioquant Image Analysis, Nashville, TN) and ImagePro Plus software (version 6.2; Media Cybernetics, Bethesda, MD) were used for image acquisition.

Statistical analysis

Two-way analysis of variance with Bonferroni *post hoc* tests was performed to assess MRI and FT-IRIS–determined parameters of repair tissue, with treatment and time point as the variables. Correlations between MRI and FT-IRIS data were assessed by the Pearson correlation. All data were analyzed in SigmaStat 3.5 software (SPSS, Chicago, IL). Statistical significance was determined at the $p \leq 0.05$ level.

Results

Magnetic resonance imaging

There was no significant difference in repair volume or morphology between TP-508 and controls at either interval. At 3 weeks, 2/34 repairs displaced (1 TP-508; 1 control). The presence of a significant increase in signal intensity in the adjacent cartilage noted in the controls compared to TP-508 ($p = 0.01$) at this time point suggests adjacent degeneration; however, this was not reflected in a regional prolongation of T2 values. Also, at 3 weeks, there was no significant difference between mean T2 of TP-508 versus placebo. At 6 weeks, there was a significant difference in T2 times with placebos, which consistently demonstrated longer T2 values ($p < 0.01$). When comparing the difference in T2 relative to hyaline cartilage in both groups, the TP-508 group was similar to control at 3 weeks, but showed a smaller difference at 6 weeks ($p = 0.01$), suggesting that the T2 values of more mature TP-508 specimens were closer to hyaline cartilage (Fig. 2 and Table 1).

Histology and FT-IRIS

Qualitative assessments. Typical FT-IRIS and histology images obtained from one tissue from each treatment group at each time point are shown in Figure 3 (histology) and Figure 4 (FT-IRIS). The histology images show evidence of

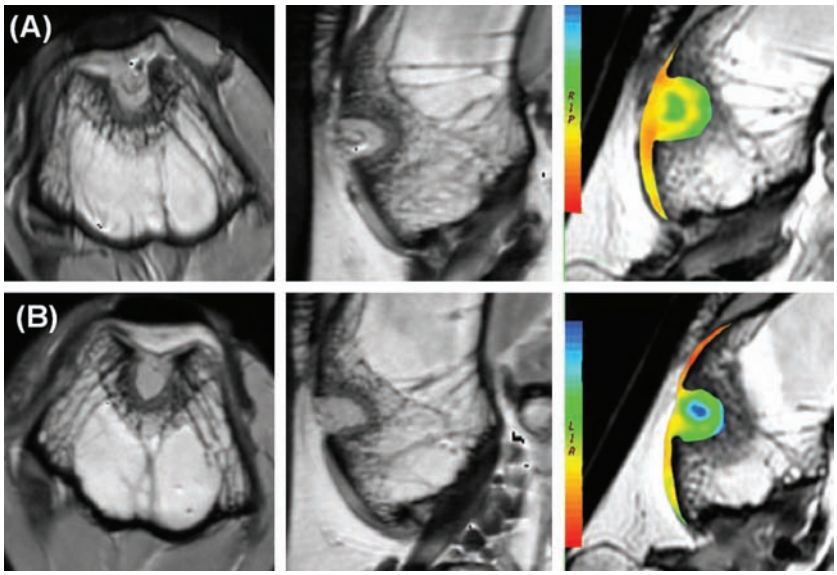

FIG. 2. Axial and saggital cartilage–sensitive fast spin echo magnetic resonance images and corresponding sagittal T2 maps demonstrating sites of cartilage repair by (**A**) thrombin peptide (TP)-508 and (**B**) placebo at 6 weeks. Color images available online at www.liebertonline.com/ten.

Table 1. Signal Intensity and T2 Relaxation Times of Repair and Native Cartilage (Mean ± Standard Deviation)

	3 weeks (n = *6*)			*6 weeks* (n = *11*)		
	TP-508	*Placebo*	p	*TP-508*	*Placebo*	p
SI repair tissue	19.8 ± 3.9	20.0 ± 4.8	0.93	20.7 ± 4.4	21.2 ± 5.3	0.78
SI native cartilage	12.6 ± 1.8	19.0 ± 5.0	**0.01**	16.7 ± 4.0	16.1 ± 3.3	0.65
T2 repair tissue	51.5 ± 17.1	61.4 ± 20.4	0.57	41.3 ± 13.2	52.0 ± 15.4	**<0.01**
T2 native cartilage	29.5 ± 3.8	31.3 ± 5.9	0.54	30.8 ± 6.3	33.1 ± 5.6	0.18
T2 difference	21.5 ± 17.1	30.8 ± 16.9	0.56	13.2 ± 8.5	21.1 ± 12.4	**0.01**

TP, thrombin peptide; SI, signal intensity.
Bold-faced numbers indicate statistical significance ($p \leq 0.01$).

the PLGA carrier degradation at the 3-week time point for both the placebo and TP-508 samples, and at the 6-week time point for the placebo sample. Repair tissue is sparse at the 3-week time point for both placebo and TP-508, but appears to increase for the TP-508 sample at 6 weeks. Comparison to native cartilage shows a clear demarcation between repair and native cartilage at both time points for both placebo and treatment. However, the TP-508 tissue has a more hyaline-like appearance at the 6-week time point.

The FT-IRIS data improve understanding of the repair process by providing molecular information on the repair tissue. It was evident that the cartilage portion of the defect region was filled with repair tissue at 6 weeks in many samples from both the TP-508 and placebo groups, as shown

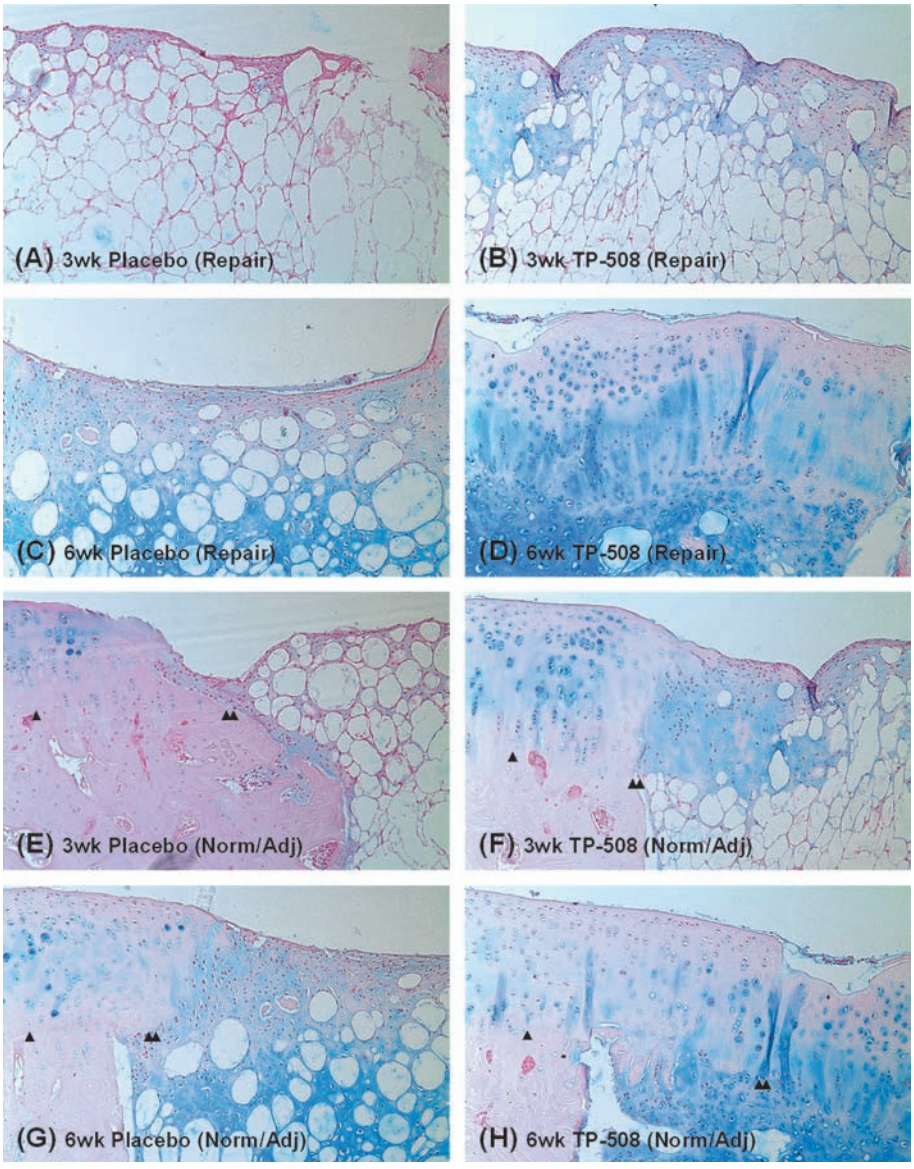

FIG. 3. Histologic images (alcian blue stain) of repair tissue and normal, adjacent cartilage (magnification, 10×). (**A**) Three-week placebo (repair), (**B**) 3-week TP-508 (repair), (**C**) 6-week placebo (repair), (**D**) 6-week TP-508 (repair), (**E**) 3-week placebo (normal/adjacent), (**F**) 3-week TP-508 (normal/adjacent), (**G**) 6-week placebo (normal/adjacent), and (**H**) 6-week TP-508 (normal/adjacent). At 3 weeks, defect fill was barely observed for both placebo and TP-508, and evidence of PLGA was present in the mesh-like structure under the articular surface. At the 6-week time point, hyaline-like repair tissue was present in the TP-508 group, but the placebo group repair tissue was more similar to fibrocartilage. Color images available online at www.liebertonline.com/ten.

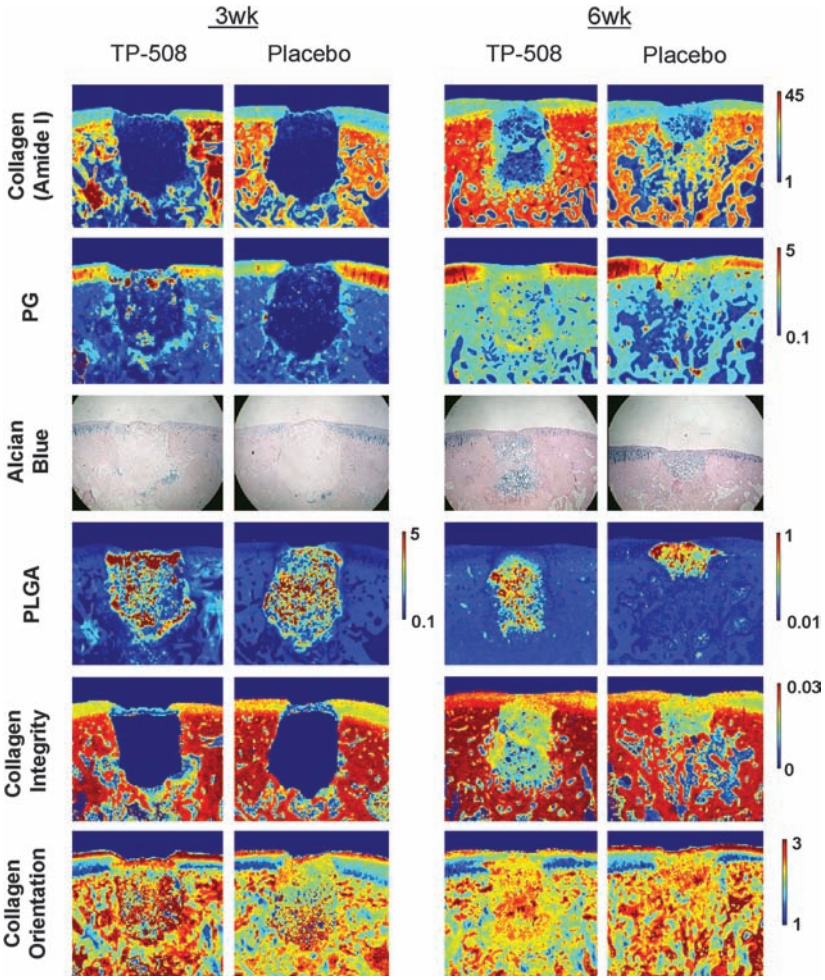

FIG. 4. Fourier transform–infrared imaging spectroscopy (FT-IRIS) images and histology of repair and adjacent normal tissue in placebo and TP-508 animals at 3 and 6 weeks postsurgery. Row 1, collagen distribution; row 2, proteoglycan (PG) distribution; row 3, alcian blue–stained histology for PG distribution (magnification, 10×); row 4, PLGA distribution (the color scale was adjusted in the 6-week group to facilitate observation of the remaining PLGA); row 5, collagen integrity; row 6, collagen orientation. In all IR images (except collagen orientation), scale bars reflect relative quantity of imaged component, where red is greatest and blue is least. For collagen orientation, red indicates fibrils parallel to the articular surface and dark blue indicates fibrils perpendicular to the articular surface. The defect region was filled with repair tissue at 6 weeks in many samples from both the TP-508 and placebo groups. Stratification of collagen fibril orientation was apparent in the normal cartilage adjacent to repair tissue in all samples, but no stratification was apparent in the repair tissue.

in the FT-IRIS Am I images. As the repair tissue filled the defect, the PLGA contribution to the defect was reduced, but not significantly. Stratification of collagen fibril orientation by cartilage zone was apparent in the normal cartilage adjacent to repair tissue in all samples, but there was no obvious stratification in the repair tissue.

Semiquantitative FT-IRIS assessments. From the 3- to 6-week time point, there was a significant increase in collagen (Am I area) in the placebo group ($p = 0.04$), in PG (PG/Am I area ratio) in the TP-508 group ($p = 0.02$), and in collagen integrity (1338 cm^{-1}/Am II area ratio) in the TP-508 group ($p = 0.002$) (Fig. 5). There were no significant differences in any repair tissue parameters between the TP-508 group and placebo group at either the 3- or 6-week time point. However, at the 3-week time point, the Am I and PG/Am I values in normal ratioed to repair tissue (normal/repair) were closer to 1 in the TP-508 group compared to placebo, indicating that the TP-508 tissue had a collagen and PG content closer to normal cartilage at the 3-week time point.

Correlation between FT-IRIS and MRI T2-mapping parameters

All normal native hyaline articular cartilage demonstrated greater FT-IRIS–determined Am I, PG, and collagen integrity parameters, and perpendicularly oriented collagen fibrils, and shorter T2 relaxation times on quantitative T2 mapping compared to repair tissue, regardless of treatment (Fig. 6A–D). Within the repair tissue groups, the 6-week TP-508 group had the shortest T2 relaxation times on average, which were closest to those of articular cartilage, and the largest mean values of FT-IRIS parameters, which were also closest to those of articular cartilage. The 3-week placebo group displayed the longest T2 relaxation times and the lowest mean values of FT-IRIS parameters, all furthest from those of normal articular cartilage. In normal native cartilage, there was a significant inverse correlation between T2 relaxation and FT-IRIS–derived collagen orientation (Fig. 6E), but no significant correlation with other FT-IRIS–determined parameters, such as PG and collagen content. In repair cartilage, there were no significant correlations between T2 relaxation and any FT-IRIS parameter (Fig. 7A–C).

Discussion

Animal models have been utilized for more than 20 years to assess cartilage repair, including various rabbit models of osteochondral defects, toward the ultimate goal of generating mechanically competent hyaline cartilage–like tissue. MRI of intact repair tissue and histological assessment of excised repair tissue are frequently used to evaluate the quality of defect fill in rabbit and other animal studies. Histological scoring systems such as that defined by O'Driscoll *et al.*[38]

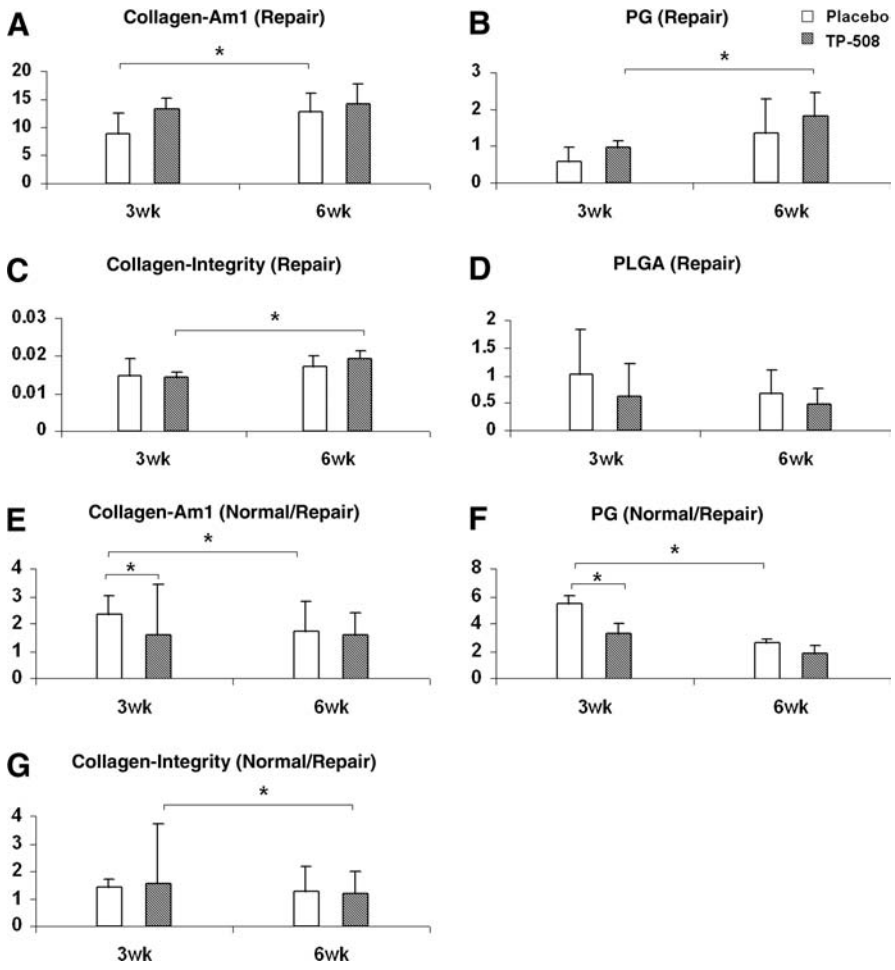

FIG. 5. Comparison of FT-IRIS parameters between placebo and TP-508 normal and repair tissue at the 3- and 6-week time points: (**A**) collagen content, (**B**) PG content, (**C**) collagen integrity, and (**D**) PLGA content (3 week, $n = 5$; 6 week, $n = 11$). Comparison of (**E**) collagen content, (**F**) PG content, and (**G**) collagen integrity values in normal cartilage ratioed to those values in repair tissue (normal/repair). The collagen and PG ratios were closer to 1 in the TP-508 tissues compared to the placebo, indicating that the TP-508 tissue had a collagen and PG content closer to normal cartilage at the 3-week time point ($^*p < 0.05$). (PLGA [normal/repair] is not available because PLGA microspheres are not present in the normal tissue.)

typically include assessment of cellular structure, tissue integration, PG staining, and cartilage thickness. Here, we demonstrated the utility of another modality, FT-IRIS imaging of repair cartilage, and correlations to MRI-derived parameters, in assessment of an osteochondral defect in the early stages of healing.

Spontaneous repair of osteochondral defects has been confirmed in several rabbit studies,[39–41] but, typically, a 12-week to 6-month interval is required for complete healing.[42] Investigation of earlier time points in the process can yield insight into mechanisms of early tissue fill, as well as alert to potential delays in healing. In the current study, MRI morphologic analysis showed no differences in defect fill at either time point, indicative of comparable healing of the TP-508 tissues compared to controls at this structural level. Given the effect of TP-508 in healing of other connective tissues,[43,44] this result is not surprising. However, since this morphologic data alone were not sufficient to discriminate the effects of TP-508 on cartilage repair compared to spontaneous repair, further analyses to investigate the biochemical and biophysical makeup of the repair tissue were performed.

MRI T2 mapping was useful in discerning effects of TP-508 compared to placebos. At 6 weeks, the TP-508 group demonstrated shorter T2 values compared to placebos, indicative of differences in repair tissue quality. Shorter T2 values arise from less water mobility in the tissue, and can reflect changes in matrix composition and structure, such as differences in collagen orientation.[45] The FT-IRIS studies performed in this study provided further information to elucidate the molecular basis for the changes that underlie the differences in the T2 values between the two repair tissues.

Until now, FT-IRIS studies of cartilage included monitoring of enzymatic collagenase degradation of cartilage,[24] evaluation of PG content in tissue-engineered cartilage,[27,28] assessment of collagen orientation in cartilage,[29] and evaluation of human and rabbit osteoarthritic (OA) cartilage tissues.[22,23,46] However, a comparison of cartilage repair tissue and native cartilage by infrared spectral analysis had not yet been undertaken. In the current study, FT-IRIS data revealed differences in the molecular composition of the repair and native tissue that likely contribute to the differences observed in T2 MRI values.

T2 values were reduced in the TP-508 repair tissue at the 6-week time point, and PG content and collagen integrity increased in the TP-508 repair tissue from 3 to 6 weeks. In comparison, the collagen content of the placebos increased from 3 to 6 weeks, with no change in PG or collagen integrity. While increased collagen content indicates growth of repair tissue in the placebo samples, the increased PG content and collagen integrity in the TP-508 samples indicate a maturation of the repair tissue. Layer stratification was not evident in repair tissue in any treatment group by polarized FT-IRIS; similarly, no discernible stratification of T2 relaxation values was evident either.

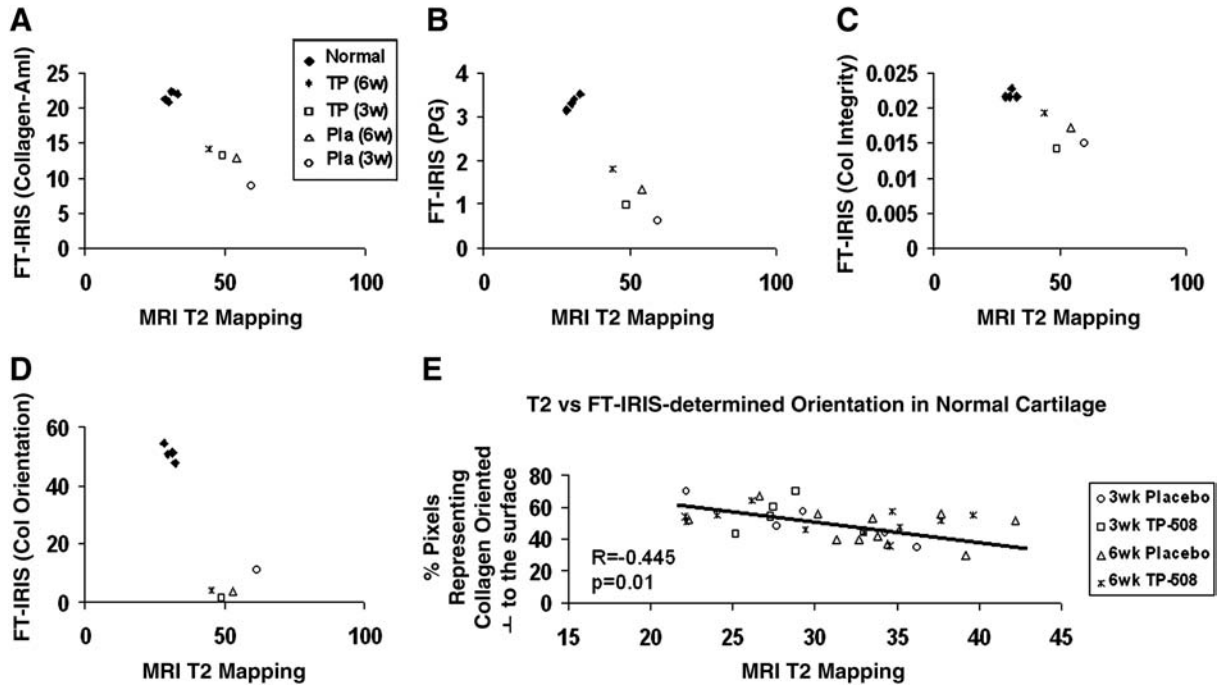

FIG. 6. Correlation between FT-IRIS–derived parameters and magnetic resonance imaging (MRI) T2 values. (**A**) T2 relaxation (ms) versus collagen–amide (Am) I content, (**B**) T2 relaxation (ms) versus PG content, (**C**) T2 relaxation (ms) versus collagen integrity (new tissue formation), and (**D**) T2 relaxation (ms) versus % pixels representing collagen fibers oriented perpendicular to the articular surface. This percentage was calculated from the polarized FT-IRIS image by dividing the pixels into three orientation categories (parallel to surface, random, and perpendicular to surface) according to Am I/Am II ratio values. The percentage of pixels falling into each category was then calculated. All normal native hyaline articular cartilage demonstrated greater FT-IRIS–determined values for Am I, PG, and collagen integrity parameters, and perpendicularly oriented collagen fibrils, and shorter T2 relaxation times compared to repair tissue, regardless of treatment. (**E**) There was a significant inverse correlation in normal cartilage between the % of pixels representing collagen oriented perpendicular to the articular surface and T2 relaxation. ◆, normal cartilage; ✕, TP-508 (6-week repair); □, TP-508 (3-week repair); △, placebo (6 week repair); ◇, placebo (3 week repair).

Repair tissue from the 6-week TP-508 group also had the FT-IRIS–derived parameters of collagen content, PG content, and collagen integrity values closest to those seen in the surrounding articular cartilage, while the values for the FT-IRIS–derived parameters of the 3-week placebo group were furthest from those of articular cartilage. Thus, both time and treatment contribute to quality of the repair. Additional analyses demonstrated no significant correlations between repair tissue T2 relaxation values and any FT-IRIS–derived parameters.

In contrast to the repair tissue, there was a significant (inverse) correlation between normal cartilage T2 relaxation values and orientation of collagen perpendicular to the articular surface, as is typically observed in the deep zone of cartilage, but no correlation to the other FT-IRIS–derived components. A recent study that assessed normal and repair cartilage in an equine model[47] also found that T2 relaxation values were correlated to orientation in normal cartilage, but that repair tissue from microfracture was disorganized and did not reflect stratification of T2. In summary, our data support the concept that T2 values in repair cartilage likely reflect matrix content, and in normal cartilage, primarily reflect matrix organization, specifically that of collagen.

A recent study from our lab utilized both FT-IRIS and MRI to assess cartilage degradation in a rabbit model of OA.[46] Reduced PG content in the OA cartilage was found by FT-IRIS, and this paralleled the MRI finding of reduced fixed charge density as assessed by a gadolinium technique. Further, a trend toward higher apparent magnetization transfer (MT) exchange rate, k_m, was also found in the OA cartilage, suggestive of changes in collagen structural features. This finding paralleled the FT-IRIS finding of altered collagen integrity. MRI analyses with gadolinium have been extremely useful in assessment of the relative amount of PG content in repair tissue in both clinical[48–50] and in preclinical studies,[51,52] but the use of magnetization transfer (MT) rate has been limited. There are also additional emerging imaging strategies to assess matrix elements, including T1 rho for PG,[53] and diffusion tensor imaging for collagen.[54]

The ability of FT-IRIS to monitor biomaterials, such as PLGA, in addition to native tissue components, is very useful in assessment of repair tissue. Knowledge of the specific time point when the carrier of a therapeutic is fully biodegraded could impact therapeutic optimization. Here, although PLGA microspheres were qualitatively reduced at the 6-week time point, they were indeed still present. Other studies have monitored the presence of PLGA microspheres in repair tissue histologically[55] and by MRI.[56] Histologically, PLGA microspheres were identified by their lack of staining in the section. FT-IRIS yields more specific data, as the molecular signature of PLGA can be utilized to identify the biomaterial based on the presence of this feature, rather than inferring the presence

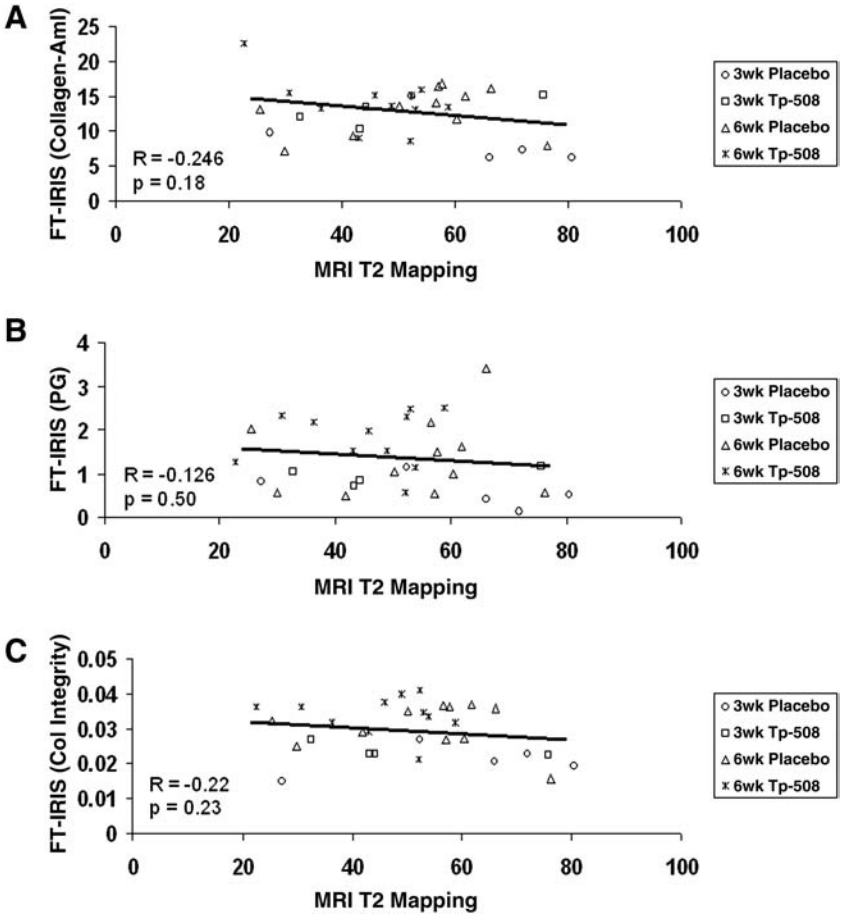

FIG. 7. Correlation between FT-IRIS–derived parameters and MRI T2 relaxation values in repair tissue. (**A**) T2 relaxation (ms) versus collagen–Am I content in repair tissue, (**B**) T2 relaxation (ms) versus PG content in repair tissue, and (**C**) T2 relaxation (ms) versus collagen integrity (new tissue formation) in repair tissue. There were no significant correlations between T2 relaxation times and the FT-IRIS–derived values in repair tissue. ×, TP-508 (6-week repair); □, TP-508 (3-week repair); △, placebo (6-week repair); ◊, placebo (3-week repair).

of PLGA based on the lack of a feature, for example, staining. In the MRI study, T2 mapping was utilized to assess cartilage repair tissue formed with and without PLGA in a rabbit osteochondral defect.[56] Although no specific data on the presence of PLGA were obtained, it was hypothesized that 4 weeks postrepair was insufficient time for the PLGA to decompose, as the T2 relaxation time increased with repair tissue depth. In our study, it is very possible that the reduced T2 relaxation time at 6 weeks could also be related to reduced PLGA content, in addition to the other tissue matrix factors previously discussed.

Despite the advantages of applying FT-IRIS to evaluate repair tissue, there are certain limitations to this modality. Specifically, in contrast to MRI, the invasiveness of this technique necessitates harvesting of the tissue for data acquisition, rather than permitting an *in situ* evaluation. Further, histological sections are dehydrated, and typically the only water that remains in the tissue is structural water. There is an alternative, however, in the infrared fiber optic probe, designed to be used arthroscopically.[22,23] Infrared fiber optic probe analysis enables determination of the molecular state of cartilage by probing the chondral surface *in situ*. However, the output is a single spectrum, and not an image. Nevertheless, molecular data can be obtained from the repair tissue site.

In summary, the current study demonstrates that local treatment with TP-508 promotes improved quality of the extracellular matrix compared to placebo in osteochondral defects. Thus, evaluation of normal and repair cartilage at the molecular level, a critical step toward optimization of therapeutic regimes, can be comprehensively addressed by utilization of MRI T2 mapping combined with FT-IRIS analysis.

Acknowledgments

This work utilized the facilities of the HSS Musculoskeletal Repair and Regeneration Core Center (NIH AR046121) and was supported by NIH EB000744 (N.P.).

Disclosure Statement

Funding for this study was provided in part by Orthologic Inc. (Tempe, AZ).

References

1. Buckwalter, J.A., and Mankin, H.J. Articular cartilage I: tissue designing and chondrocyte matrix interactions. J Bone Joint Surg **79A,** 600, 1997.
2. Brandt, K.D., Doherty, M., and Lohmander, L.S. Composition and structure of articular cartilage. Osteoarthritis. New York: Oxford University Press Inc., 1998.
3. Mankin, H.J. The response of articular cartilage to mechanical injury. J Bone Joint Surg **64,** 460, 1982.
4. Newman, A.P. Articular cartilage repair. Am J Sports Med **26,** 309, 1998.
5. Freed, L.E., Grande, D.A., Lingbin, Z., Emmanual, J., Marquis, J.C., and Langer, R. Joint resurfacing using allograft chondrocytes and synthetic biodegradable polymer scaffolds. J Biomed Mater Res **48,** 891, 1994.

6. Shortkroff, S., Barone, L., Hsu, H.P., Wrenn, C., Gagne, T., Chi, T., Breinan, H., Minas, T., Sledge, C.B., Tubo, R., and Spector, M. Healing of chondral and osteochondral defects in a canine model: the role of cultured chondrocytes in regeneration of articular cartilage. Biomaterials **17,** 147, 1996.
7. Sims, C.D., Butler, P.E., Cao, Y.L., Casanova, R., Randolph, M.A., Black, A., Vacanti, C.A., and Yaremchuck, M.J. Tissue engineered neocartilage using plasma derived polymer substrates and chondrocytes. Plast Reconstr Surg **101,** 1580, 1998.
8. Grande, D.A., Pitman, M.I., Peterson, L., Menche, D., and Klein, M. The repair of experimentally produced defects in rabbit articular cartilage by autologous chondrycyte transplantation. J Orthop Res **7,** 208, 2005.
9. Hoikka, V.E., Jaroma, H.J., and Ritsila, V.A. Reconstruction of the patellar articulation with periosteal grafts, 4-year follow-up of 13 cases. Acta Orthop Scand **61,** 36, 1990.
10. Emans, P.J., Hulsbosch, M., Wetzels, G.M, Bulstra, S.K., and Kuijer, R. Repair of osteochondral defects in rabbits with ectopically produced cartilage. Tissue Eng **11,** 1789, 2005.
11. Homminga, G.N., Bulsrta, S.K., Bouwmeeter, P.S., and van der Linden, A.J. Perichondrial grafting for cartilage lesions of the knee. J Bone Joint Surg **72,** 1003, 1990.
12. Chu, C.R., Coutts, RD., Yoshioka, M., Harwood, F.L., Monosov, A.Z., and Amiel, D. Articular cartilage repair using collagen allogenic perichondrocyte-seeded biodegradable porous acid (PLA): a tissue-engineering study. J Biomed Mater Res **29,** 1147, 1995.
13. Wakitani, S., Kimura, T., Hirooka, A., Ochi, T., Yoneda, M., Yasui, N., Owaki, H., and Ono, K. Repair of rabbit articular surfaces with allograft chondrocytes embedded in collagen gel. J Bone Joint Surg **71,** 74, 1989.
14. Goldberg, A. Effects of growth factors on articular cartilage. Orthop Traumatol Rehabil **3,** 209, 2001.
15. Blaney Davidson, E.N., Vitters, E.L., van Lent, P.L., van de Loo, F.A., van der Berg, W.B., and van der Kraan, P.M. Elevated extracellular matrix production and degradation upon bone morphogenetic protein-2 (BMP-2) stimulation point toward a role for BMP-2 in cartilage repair and remodeling. Arthritis Res Ther **9,** R102, 2007.
16. Howard, R.D., Mc Ilwraith, C.W., Trotter, G.W., Powers, B.E., McFadden, P.R., Harwood, F.L., and Amiel, D. Long-term fate and effects of exercise on sternal cartilage autographs used for repair of large osteochondral defects in horses. Am J Vet Res **55,** 1158, 1994.
17. Voloshin, I., DeHaven, K.E., and Steadman, J.R. Second-look arthroscopic observations after radiofrequency treatment of partial thickness articular cartilage defects in human knees: report of four cases. J Knee Surg **18,** 116, 2005.
18. Potter, H.G., Linklater, J.M., Allen, A.A., Hanafin, J.A., and Haas, S.B. Magnetic resonance imaging of articular cartilage in the knee. An evaluation with use of fast-spin echo imaging. J Bone Joint Surg **80,** 1276, 1998.
19. Marlovits, S., Singer, P., Zeller, P., Mandle, I., Haller, J., and Trattnig, S. Magnetic resonance observation of cartilage repair tissue (MOCART) for the evaluation of autologous chondrocyte transplantation: determination of interobserver variability and correlation to clinical outcome after 2 years. Eur J Radiol **57,** 16, 2006.
20. Xia, Y. Averaged and depth-dependent aniotropy of articular cartilage by microscopic imaging. Semin Arthritis Rheum **37,** 317, 2008.
21. Camacho, N.P., West, P.A., Torzilli, P.A., and Mendelsohn, R. FTIR microscopic imaging of collagen and proteoglycan in bovine cartilage. Biopolymers **62,** 1, 2001.
22. West, P.A., Bostrom, M.P., Torzilli, P.A., and Camacho, N.P. Fourier transform infrared spectral analysis of degenerative cartilage: an infrared fiber optic probe and imaging study. Appl Spectrosc **58,** 376, 2004.
23. Li, G., Thomson, M., Decarlo, E., Yang, X., Nester, B., Bostrom, M.P., and Camacho, N.P. A chemometric analysis for evaluation of early-stage cartilage degradation by infrared fiber-optic probe spectroscopy. Appl Spectrosc **59,** 1527, 2005.
24. West, P.A., Torzilli, P.A., Chen, C., Lin, P., and Camacho, N.P. Fourier transform infrared imaging spectroscopy analysis of collagenase-induced cartilage degradation. J Biomed Opt **10,** 14015, 2005.
25. Anderson, H.C., Sipe, J.B., Hessle, L., Dhanyamraju, R., Atti, E., Camacho, N.P., and Millan, J.L. Impaired calcification around matrix vesicles of growth plate and bone in alkaline phosphate-deficient mice. Am J Pathol **164,** 841, 2004.
26. Boskey, A.L. Assessment of bone mineral and matrix using backscatter electron imaging and FTIR imaging. Curr Osteoporos Rep **4,** 71, 2006.
27. Kim, M., Bi, X., Horton, W.E., Spencer, R.G., and Camacho, N.P. Fourier transform infrared imaging spectroscopic analysis of tissue engineered cartilage: histologic and biochemical correlations. J Biomed Opt **10,** 031105, 2005.
28. Boskey, A.L., and Pleshko Camacho, N. FT-IR imaging of native and tissue-engineered bone and cartilage. Biomaterials **28,** 1050, 2007.
29. Bi, X., Li, G., Doty, S.B., and Camacho, N.P. A novel method for determination of collagen orientation in cartilage by Fourier transform infrared imaging spectroscopy (FT-IRIS). Osteoarthritis Cartilage **13,** 1050, 2005.
30. Rudert, M., Wilms, U., Hoberg, M., and Wirth, C.J. Cell-based treatment of osteochondral defects in the rabbit knee with natural and synthetic matrices: cellular seeding determines the outcome. Arch Orthop Trauma Surg **125,** 598, 2005.
31. Carney, D.H., Mann, R., Redin, W.R., Pernia, S.D., Berry, D., Heggers, J.P., Hayward, P.G., Robson, M.C., Christie, J., and Annable, C. Enhancement of incisional wound healing and neovascularization in normal rats by thrombin and synthetic thrombin receptor-activating peptides. J Clin Invest **89,** 1469, 1992.
32. Hallberg, C., and Gill, K. Enhancement of corneal ephithelial wound healing by thrombin recepter activating peptide in the rat. Res Commun Pharmacol Toxicol **2,** 129, 1997.
33. Simmons, D.J., Yang, J., and Yang, S. "Acceleration of Rat Femoral Fracture Healing by a Synthetic Thrombin Peptide," In: C. Dacke, J. Danks, G. Glik and C. Gay, eds. Calcium Metabolism: Comparative Endocrinology. Proc Satellite Meeting, San Francisco, CA. Nov. 30, 1998. BioScientifica Ltd. Bradley Stoke, Bristol, UK. 1999. pp. 1–15.
34. Glenn, K.C., Frost, G.H., Bergmann, J.S., and Carney, D.H. Synthetic peptides bind to high-affinity thrombin receptors and modulate thrombin mitogenesis. Pept Res **1,** 65, 1988.
35. Glenn, R.E.J., Mc Carty, E.C., Potter, H.G., Juliao, S.F., Gordon, J.D., and Spindler, K.P. Comparison of fresh osteochondral autografts and allografts: a canine model. Am J Sports Med **34,** 1084, 2006.
36. Maier, C.F., Tan, S.G., Hariharan, H., and Potter, H.G. T2 quantitation of articular cartilage at 1.5T. J Mag Reson Imaging **17,** 358, 2003.
37. Ippolito, E., Pedrini, V.A., and Pedrini-Mille, A. Histochemical properties of cartilage proteoglycans. J Histochem Cytochem **31,** 53, 1983.

38. O'Driscoll, S.W., Marx, R.G., Beaton, D.E., Miura, Y., Gallay, S.H., and Fitzsimmons, J.S. Validation of a sample histological-histochemical cartilage scoring system. Tissue Eng **7,** 313, 2001.
39. Frenkel, S.R., Bradica, G., Brekke, J.H., Goldman, S.M., Ieska, K., Issack, P., Bong, M.R., Tian, H., Gokhale, J., Coutts, R.D., and Kronengold, R.T. Regeneration of articular cartilage—evaluation of osteochondral defect repair in the rabbit using multiphasic implants. Osteoarthritis Cartilage **13,** 798, 2005.
40. Huang, X., Yang, D., Yan, W., Shi, Z., Feng, J., Gao, Y., Weng, W., and Yan, S. Osteochondral repair using the combination of fibroblast growth factor and amorphous calcium phosphate/poly(L-lactic acid) hybrid materials. Biomaterials **28,** 3091, 2007.
41. Filova, E., Jelinek, F., Handl, M., Lytvynets, A., Rampichova, M., Varga, F., Cinati, J., Soukup, T., Trc, T., and Amler, E. Novel composite hyaluronan/type I collagen/fibrin scaffold enhances repair of osteochondral defect in rabbit knee. J Biomed Mater Res B Appl Biomater **87,** 415, 2008.
42. Rudert, M. Histological evaluation of osteochondral defects: consideration of animal models with emphasis on the rabbit, experimental setup, follow-up and applied methods. Cells Tissues Organs **171,** 229, 2002.
43. Schwartz, Z., Carney, D.H., Crowther, R.S., Ryaby, J.T., and Boyan, B.D. Thrombin peptide (TP-508) treatment of rat growth plate cartilage cells promotes proliferation and retention of the chondrocytic phenotype while blocking terminal endochondral differentiation. J Cell Physiol **202,** 336, 2005.
44. Stiernberg, J., Norfleet, A.M., Redin, W.R., Warner, W.S., Fritz, R.R., and Carney, D.H. Acceleration of full-thickness wound healing in normal rats by the synthetic thrombin peptide, TP-508. Wound Repair Regen **8,** 204, 2000.
45. Potter, H.G., and Foo, L.F. Magnetic resonance imaging of articular cartilage: trauma, degeneration, and repair. Am J Sports Med **34,** 317, 2006.
46. Bi, X., Yang, X., Bostrom, M.P., Bartusik, D., Ramaswamy, S., Fishbein, K.W., Spencer, R.G., and Camacho, N.P. Fourier transform infrared imaging and MR microscopy studies detect compositional and structural changes in cartilage in a rabbit model of osteoarthritis. Anal Bioanal Chem **387,** 1601, 2007.
47. White, L.M., Sussman, M.S., Hurtig, M., Probyn, L., Tomlinson, G., and Kandel, R. Cartilage T2 assessment: differentiation of normal hyaline cartilage and reparative tissue after arthroscopic cartilage repair in equine subjects. Radiology **241,** 407, 2006.
48. Vasara, A.I., Nieminen, M.T., Jurvelin, J.S., Peterson, L., Lindahl, A., and Kiviranta, I. Indentation stiffness of repair tissue after autologous chondrocyte transplantation. Clin Orthop Relat Res **433,** 233, 2005.
49. Ling, W., Regatte, R.R., Navon, G., and Jerschow, A. Assessment of glycosaminoglycan concentration *in vivo* by chemical exchange-dependent saturation transfer (gagCEST). Proc Natl Acad Sci USA **105,** 2266, 2008.
50. Trattnig, S., Manisch, T.C., Pinker, K., Domayer, S., Szomolanyi, P., Marlovits, S., Kutscha-Lissberg, F., and Welsch, G.H. Differentiating normal hyaline cartilage from post-surgical repair tissue using fact gradient echo imaging in delayed gadolinium-enhanced MRI (dGEMRIC) at 3 Tesla. Eur Radiol **18,** 1251, 2008.
51. Hicks, C.R., Morris, I.T., Vijayasekaran, S., Fallon, M.J., McAllister, J., Clayton, A.B., Chirila, T.V., Crawford, G.J., and Constable, I.J. Correlation of histological findings with gadolinium enhanced MRI scans during healing of a PHEMA orbital implant in rabbits. Br J Opththalmol **83,** 616, 1999.
52. Williams, A., Oppenheimer, R.A., Gray, M.L., and Burstein, D. Differential recovery of glycosaminoglycan after IL-1-induced degradation of bovine articular cartilage depends on degree of degradation. Arthritis Res Ther **5,** R97, 2003.
53. Wheaton, A.J., Dodge, G.R., Borthakur, A., Kneeland, J.B., Schumacher, H.R., and Reddy, R. Detection of changes in articular cartilage proteoglycan by T(1rho) magnetic resonance imaging. J Orthop Res **23,** 102, 2005.
54. de Visser, S.K., Bowden, J.C., Wentrup-Byrne, E., Rintoul, L., Bostrom, T., Pope, J.M., and Momot, K.I. Anisotropy of collagen fibre alignment in bovine cartilage: comparison of polarized light microscopy and spatially resolved diffusion-tensor measurements. Osteoarthritis Cartilage **16,** 689, 2008.
55. Kang, S.W., Yoon, J.R., Lee, J.S., Kim, H.J., Lim, H.C., Park, J.H., and Kim, B.S. The use of poly (lactic-co-glycolic acid) microspheres as injectable cell carriers for cartilage regeneration in rabbit knees. J Biomater Sci Polym Ed **17,** 925, 2006.
56. Zalewski, T., Lubiatowski, P., Jaroszewski, J., Szczesniak, E., Kusmia, S., Kruczynski, J., and Jurga, S. Scaffold-aided repair of articular cartilage studied by MRI. MAGMA **21,** 177, 2008.

Address correspondence to:
Nancy Pleshko, Ph.D.
Dept. of Mechanical Engineering
Temple University
1947 N. 12th St.
Philadelphia, PA 19104

E-mail: npleshko@temple.edu

Received: January 9, 2009
Accepted: July 7, 2009
Online Publication Date: October 21, 2009